The Effect of Water on the Rate of Conformational Change in Protein Allostery

Robert A. Goldbeck, Sarah J. Paquette, and David S. Kliger
Department of Chemistry and Biochemistry, University of California, Santa Cruz, California 95064 USA

ABSTRACT The influence of solvation on the rate of quaternary structural change is investigated in human hemoglobin, an allosteric protein in which reduced water activity destabilizes the R state relative to T. Nanosecond absorption spectroscopy of the heme Soret band was used to monitor protein relaxation after photodissociation of aqueous HbCO complex under osmotic stress induced by the nonbinding cosolute poly(ethylene glycol) (PEG). Photolysis data were analyzed globally for six exponential time constants and amplitudes as a function of osmotic stress and viscosity. Increases in time constants associated with geminate rebinding, tertiary relaxation, and quaternary relaxation were observed in the presence of PEG, along with a decrease in the fraction of hemes rebinding CO with the slow rate constant characteristic of the T state. An analysis of these results along with those obtained by others for small cosolutes showed that both osmotic stress and solvent viscosity are important determinants of the microscopic R $\rightarrow$ T rate constant. The size and direction of the osmotic stress effect suggests that at least nine additional water molecules are required to solvate the allosteric transition state relative to the R-state hydration, implying that the transition state has a greater solvent-exposed area than either end state.

INTRODUCTION

The activity of water, a ubiquitous solvent in biochemical studies, is often assumed to be a constant that can be safely ignored. However, its activity is lowered in living cells from that of pure water by the presence of solutes, typically at concentrations high enough to produce an osmotic pressure of $\sim$7 atm (Stock et al., 1977). Because of the large contribution of solvation to the stability of a protein, lowering the activity of water can affect the thermodynamics and kinetics of reactions that alter the protein's solvent-exposed surface area. Consequently, perturbing solvent activity can be a useful tool for obtaining structural information about reaction end states and transition states, and for assessing the physiological relevance of biochemical studies (Parsegian et al., 1994, 1995; LiCata and Allewell, 1998).

In the present work we explore the influence of water activity on the rate of structural relaxation in human hemoglobin, an oxygen transport protein comprising two pairs of heme-polypeptide chains, $\alpha_1\beta_1$ and $\alpha_2\beta_2$, bound in a roughly spherical dimer of dimers. Hemoglobin serves as a prototypical example of allostery, the interaction between ligand binding at an active site and the properties of other active sites in a protein providing for the regulation of function in response to changing physiological conditions. Because conformational motions of the polypeptide backbone and residue side chains may expose varying amounts of protein surface to the solvent during progress along the allosteric reaction pathway, the results of kinetic osmotic stress studies are expected to yield information about the role of water binding in stabilizing transition states in protein allostery, information that can in turn shed light on the physical nature of the transition states and their kinetic mechanisms.

The role of solvation in allostery has long been recognized in principle, but only recently has it been studied explicitly. Moreover, previous studies have focused on reaction end states, leaving the role of water in the dynamics of allostery largely unexplored. Equilibrium studies have used osmotic stress methods to examine the hydration changes accompanying structural differences between allosteric states, particularly differences in the solvent-exposed surface area of proteins (Parsegian et al., 1995). Colombo et al. (1992) applied equilibrium osmotic stress methods to study allostery in human hemoglobin, in which four heme prosthetic groups cooperate to bind O_2 with different affinities under different physiological conditions—high affinity in oxygen-rich pulmonary capillaries and lowered affinity in oxygen-poor tissue capillaries—by communicating changes in their iron atom's axial ligation state between subunits. This communication is mediated by the coupling of ligation-induced tertiary alterations within subunits to a conformational equilibrium between low-affinity T and high-affinity R quaternary states (Perutz, 1992). Hemoglobin's allosteric equilibrium is further regulated by the binding of small effector molecules and ions such as H^+, CO_2, Cl^-, and phosphates. Colombo et al. (1992) showed that water can be added to this list in the sense that its activity also appears to influence the allosteric equilibrium. They found that more oxygen tension is needed for hemoglobin to reach half of binding saturation when sugar and polyol cosolutes such as sucrose, stachylose, and poly(ethylene glycol) (PEG) are present, an effect that is not observed for the monomer myoglobin. Plots of the log of the relative shift in oxygen partial pressure at half-saturation, $\log(p_{50}/p_{50}^0)$, versus the log of the increase in cosolute molar concentration

Received for publication 16 January 2001 and in final form 26 June 2001.
Address reprint requests to Dr. Robert A. Goldbeck, Dept. of Chemistry and Biochemistry, Thimann Labs., University of California, Santa Cruz, CA 95064. Tel.: 831-459-4007; Fax: 831-459-2935; E-mail: goldbeck@chemistry.ucsc.edu.

0006-3495/01/11/2919/16 $2.00

were nonlinear, evidence that the reduction in O_2 affinity was not due to direct binding of these cosolutes to hemoglobin (Arakawa and Timasheff, 1982). In contrast, plots of $\log(p_{50}/p_{50}^0)$ versus the log of osmotic pressure (Π) were linear and superimposable for different cosolutes, indicating that the osmolality of a cosolute and not its chemical structure was responsible for lowering O_2 affinity (Colombo et al., 1992). Those results underlie the idea that osmolytes can modulate O_2 affinity indirectly through the solvent chemical potential, i.e., by shifting the R $\leftrightarrow$ T equilibrium in response to decreased protein hydration (Parsegian et al., 1995).

Colombo et al. calculated from the slope of $\log(p_{50}/p_{50}^0)$ versus $\log(\Pi)$ that $\sim$60 additional H_2O molecules are bound in hydrating hemoglobin's R conformer relative to T (0.1 M NaCl/0.05 M Tris-HC1 buffer, pH 6.93, 37°C), a number that is in rough agreement with that expected from estimates of the difference in solvent-exposed areas between the R and T states, 500–800 Å^2 (Lesk et al., 1985), and the expected covering area of a single water molecule, 7–10 Å^2. The osmotic work measured during equilibrium oxygen binding represents the energy required to transfer these $\sim$60 H_2O molecules from the bulk solution to additional protein surface exposed in the R state, the less hydrated T structure thus being energetically more favored in the presence of osmolytes.

PEG is a hydrophilic polyether and is repelled by charged amino acid residues, particularly negatively charged residues (Lee and Lee, 1981). The preferential binding parameter, a quantity that expresses the relative affinities of solvent components (PEG vs. H_2O) for protein surfaces, is negative for the interaction of PEG with many globular proteins (Arakawa and Timasheff, 1985). PEG thus tends to be excluded from the layer of water molecules near the protein surface. As a cosolute, PEG is expected to reduce the activity of these vicinal waters through osmotic pressure, forcing water molecules to migrate from solvent-exposed surfaces, interfacial surfaces, and internal clefts into the bulk solution (Parsegian et al., 1994). Consistent with an osmotic mechanism, identical osmolalities of PEG-400 and PEG-150 are observed to similarly perturb equilibrium oxygen binding (Colombo et al., 1992).

To investigate the kinetic implications of water activity in hemoglobin allostery, we studied the effect of PEG osmolyte on relaxation time constants previously reported in multichannel absorption measurements by our laboratory (Shapiro et al., 1995; Goldbeck et al., 1996) and others (Hofrichter et al., 1983) for the photodissociation reactions of HbCO. Previous time-resolved studies explicitly addressing the effect of osmotic stress on allosteric proteins appear to be generally lacking, although Mitchell and Litman (1999) have measured the effect of osmotic stress on a conformational relaxation rate in rhodopsin, observing a reduction in the rate of the transition from the metarhodopsin I to the metarhodopsin II photointermediate. The hemoglobin results presented here show that PEG perturbs the time constants for tertiary and quaternary conformational relaxations measured after CO photodissociation. Both osmotic stress and viscosity are found to play a role in these changes. By analyzing these data along with data from Sawicki and Khaleque (1983), who conducted a viscosity study of hemoglobin with sugar and small polyol cosolutes, we are able to disentangle the manner in which water activity and viscosity affect the R $\rightarrow$ T relaxation kinetics. The results for the effect of water activity yield new information about the structure of the allosteric transition state, which we discuss in the context of theoretical models such as the reaction pathway of Janin and Wodak (1985).

EXPERIMENTAL

Sample preparation

Human hemoglobin was collected from venous blood [from the same non-smoking donor as used in our previous studies (Goldbeck et al., 1996)], treated with citrate anticoagulant, and prepared at 4°C according to published procedures (Geraci et al., 1969). After withdrawing most of the plasma by pipette, the serum albumin and other small proteins were removed by rinsing the red cells with three volumes of chilled 1% saline solution. Centrifugation at 4000 rpm for 4 min at 20°C followed each wash. Gentle mixing of a volume of erythrocytes with an equal volume of chilled water lysed the red cell membranes. The released hemoglobin tetramers were separated from the stromata by pipette and centrifuged at 10,000 rpm for 30 min at 4°C to remove the leukocyte pellet. The hemosylate was immediately dialyzed in the cold over 48 h against a 0.1-M sodium phosphate buffer [without using column chromatography to strip small ions and the organic phosphate, 2,3-diphosphoglycerate (DPG)]. Because the solution was not passed through a mixed-bed ion exchange resin, the UV-vis spectra showed the expected percentage (1.5–3%) of metHb (Antinoni and Brunori, 1971). Frozen pellets obtained by pipetting small droplets of the hemosylate into liquid nitrogen were stored at −80°C.

Poly(ethylene glycol) with an average molecular weight of 200 (PEG-200, 5% water content) was used as a cosolute in the HbCO sample solutions. Analytical grade sodium phosphate was used to prepare aqueous solutions of low ionic strength (0.1 M) buffered at pH 7.3 (NaH_2PO_4 + Na_2HPO_4). Dilution of PEG-200 into the sodium phosphate buffer stock gave polymer solutions of 10, 20, and 30 percent by weight to induce osmotic pressures of $\sim$13, 25, and 38 atm, respectively, as estimated from $\Pi = RTc_M$ (c_M, the concentration in moles/liter, is approximated here by the molality). The concentrated Hb pellets were dissolved into these buffered polymer stock solutions. Overnight bubbling with hydrated CO ensured complete saturation of the PEG solutions before dilution of the concentrated Hb pellets. Filters of 0.2-μm pore size and 300-nm diameter were used to remove impurities from the PEG-HbCO solutions, which were prepared to a final concentration of 120 μM heme based on a millimolar extinction coefficient of 13.4 at 569 nm. This concentration is high enough that dimer formation is $\leqslant$10% (Antinoni and Brunori, 1971), but low enough to provide a maximum Soret region (400–470 nm) absorption of $\sim$1 in a 0.5-mm path length cuvette. The PEG-Hb solutions were purged with hydrated CO in the oxygen-free experimental apparatus for 15 min before initiation of the experiment to complete formation of the carbonyl complex. A small excess of dithionite reductant solution, prepared with deoxygenated buffer, was also injected anaerobically just before measurements to ensure the ferrous oxidation state. The viscosity of the buffered PEG-Hb solutions was measured using a Ubbelohde-type capillary viscometer maintained at constant temperature to within $\pm$0.01°C.

Spectral measurements

The time-resolved absorbance spectra were measured on a laser photolysis apparatus described previously (Lewis et al., 1987). All samples were photolyzed by 7-ns (FWHM), 15-mJ laser pulses of second harmonic (532-nm) light from a Nd:YAG laser. The pump wavelength was absorbed by the Q-bands, porphyrin $\pi \rightarrow \pi^*$ absorption bands near 540 nm overlapping the excitation wavelength (Antinoni and Brunori, 1971). Absorbance changes after photodissociation were probed as a function of time with a pulsed short-arc xenon flashlamp. The transmitted light was dispersed by a spectrograph and detected with an optical multichannel analyzer (OMA) whose 10-ns gate was controlled by a pulse amplifier. An entrance slit width of 100 μm on the spectrograph provided spectral resolution of ~2 nm. Timing among the laser Q-switch, flashlamp, and the pulsed detector was controlled by a multichannel digital delay generator. Zero time was defined by the maximum laser scatter measured by the OMA at 532 nm. The vertically polarized laser beam entered the sample at a 30° incident angle to the flashlamp probe beam, which was polarized at magic angle (54.7°) relative to the actinic polarization to eliminate artifacts due to molecular rotation (Kliger et al., 1990). Control measurements performed with the flashlamp probe polarized either parallel, $\Delta A_{\parallel}$, or perpendicular, $\Delta A_{\perp}$, to that of the photolysis pulse were used to calculate an isotropic average data set. Time constants resulting from kinetic analysis of the isotropic average data set were equivalent to those recorded at magic angle.

Each transient difference spectrum was calculated by taking the log of the ratio of the probe intensity recorded by the OMA in the absence of a photolysis pulse to the intensity measured for the photolyzed sample. Continuous laser irradiation during each sample run was avoided by slowly flowing the HbCO/PEG solution in a closed system. A small Teflon stopcock provided control over the gravity flow of a 40-ml aliquot from an upper reservoir through the optical cuvette, maintained at 20°C by a recirculating water bath, into the bottom reservoir. When the upper reservoir emptied, the inlet CO pressure was adjusted to recycle the HbCO sample back up for another set of measurements. Identical spectra recorded at 16 ns after photolysis confirmed sample integrity between successive experimental measurements.

Spectral measurements were obtained at 71 logarithmically spaced delay times extending from 16 ns to 90 ms, ~10 points in each time decade. In the nanosecond time regime, 17 probe times were recorded between 16 ns and 100 ns; in the microsecond time regime, 30 probe times were recorded between 1 μs and 800 μs; and in the millisecond time regime, 24 probe times were recorded between 1 ms and 90 ms. Averaging signals measured over six separate experiments produced a total of 852 averages at each PEG-200 concentration. Because the pH of the sample solutions increased as a function of increasing PEG concentration, data obtained in PEG-free solutions at similar pH values were included in the analyses as a pH control to facilitate interpretation of PEG-induced kinetic effects.

Singular value decomposition

The photolysis data consist of a two-dimensional matrix of absorbance changes recorded at 115 wavelengths from 400 to 470 nm at each of the 71 probe times. Kinetic analysis of large data arrays is simplified by singular value decomposition (SVD) of the spectral difference matrix. This approach isolates the significant spectrokinetically independent components of the data for global fitting to a sum of exponential decays (Henry and Hofrichter, 1992; Goldbeck and Kliger, 1993). The original two-dimensional array of absorbance changes **A** is represented as the product of three matrices, **U**, **S**, and **V**.

$$\mathbf{A} = \mathbf{USV}^{\mathrm{T}} \tag{1}$$

The matrix **A** contains m rows, one for each wavelength, and n columns, one for each probe time. The $m \times n$ matrices, **U** and **V**, each consist of columns of orthonormal vectors and **S** is an $n \times n$ diagonal matrix. The 115-element columns of **U**, referred to as basis spectra, are the output of the SVD and are composed of linear combinations of the difference spectra of the physical spectrokinetic components contributing to **A**. The corresponding time courses, the 71-element columns of **V**, are linear combinations of the time courses of the physical components. The elements of **V** are used as input for the global fitting procedure. The matrix **S** contains the singular values of **A**, nonnegative diagonal elements whose values are arranged in order of decreasing magnitude. The columns of **U**, ordered correspondingly, reflect the relative contribution of each basis spectrum to the data. The best approximation to **A** using n basis components as described by Eq. 1 is the product of the first n columns of **U**, the first n rows of $\mathbf{V}^{\mathrm{T}}$, and the $n \times n$ upper-left-hand-corner of **S**. The smallest value of n for which the spectrokinetic information contained in the truncated representation is equivalent to that in the entire data set is the rank of the data matrix, the components corresponding to higher values of n containing essentially experimental noise. No further noise reduction procedures, e.g., offsetting or smoothing algorithms, beyond the SVD were applied to the data.

Kinetic analysis

A simplex algorithm was used to obtain observed time constants for kinetic intermediates by fitting multiple exponential decays to the columns of **V**. At a concentration of 1 mM free CO, the bimolecular CO recombination reaction follows pseudo-first-order kinetics. Associated with each time constant (τ_i) is an amplitude value (A_i) that reflects the relative importance of each spectral process to the overall photointermediate difference spectra. The value of the residuals between the photolysis data and the global fit, squared and summed over all wavelengths and times, was minimized in the exponential fitting program.

RESULTS

Fig. 1 *A* shows the time evolution of the hemoglobin photolysis difference spectrum after CO photodissociation in pH 7.3 buffer solution at 20°C, unperturbed by the presence of PEG cosolute. The dominant features are a partial decay of the photolysis difference intensity at early times, corresponding to geminate recombination of CO ligand, and the final completion of intensity decay, corresponding to bimolecular CO recombination, after a plateau between the two ligand-recombination time regimes. During the plateau, which extends from ~1 μs to ~100 μs after photolysis, small evolutions in spectral bandshape can be detected corresponding to the protein conformational relaxations associated with allostery.

The spectral evolution perturbed by the presence of 30% (w/w) PEG-200 is shown in Fig. 1 *B*. Although the effect of PEG is subtle enough that the two sets of difference spectra appear very similar, a small decrease in the amplitude of the photolysis signal remaining at the latest times can be seen in the PEG-perturbed evolution. This drop in amplitude will be used in conjunction with changes in relaxation time constants to calculate the allosteric R $\rightarrow$ T transition rate constant as a function of PEG concentration, as explained further below.

The six time constants and global amplitudes shown in Table 1 for PEG-free HbCO are identical within experimental error to those reported previously by this laboratory

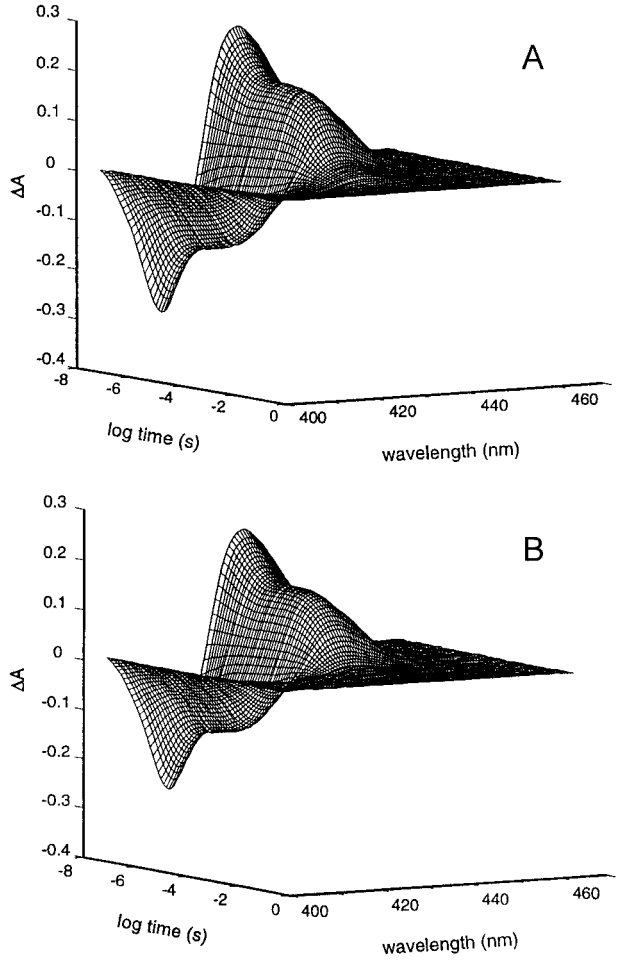

FIGURE 1 Time-resolved Soret band absorption of HbCO solution after CO photolysis at 20°C, pH 7.3. (*A*) PEG-free; (*B*) 30% PEG-200.

(Goldbeck et al., 1996) and are very similar to the results of global kinetic analyses reported by others (Hofrichter et al., 1983; Murray et al., 1988). The earliest process, taking place in tens of nanoseconds, has been assigned to geminate recombination of CO ligand that has not escaped from the protein matrix (Alpert et al., 1979; Duddell et al., 1979; Friedman and Lyons, 1980). The second time constant is conventionally assigned to a relaxation of protein tertiary structure at the heme pocket observed in time-resolved resonance Raman spectra (Friedman et al., 1982). However, a recent absorption study has shown that most of the spectral amplitude of this process can be assigned to a second geminate recombination process with a time constant of ~160 ns (Esquerra et al., 2000), overlapping the time course of the tertiary relaxation. The third time constant, $\tau_3 \sim 1\ \mu s$, has been tentatively assigned in previous studies to additional tertiary relaxation at the heme pocket (Murray et al., 1988), but there is increasing evidence from near-UV time-resolved resonance Raman (Rodgers et al., 1992) and circular dichroism (Björling et al., 1996) spectroscopies that this process also involves a relaxation of dimer-dimer contacts at ~1 μs after photolysis constituting the first step in a compound mechanism for the quaternary transition (Jayaraman et al., 1995; Goldbeck et al., 1996). Process 4, occurring tens of microseconds after photolysis, is conventionally assigned to the R → T quaternary structural transition, an assignment based on the pioneering photolysis studies of Sawicki and Gibson (1976), although the emerging characterization of process 3 as a quaternary relaxation implies that process 4 is more precisely regarded as the rate-limiting step along a compound R → T pathway. It should also be kept in mind that the observed time constant for process 4 actually reflects a kinetic competition between structural relaxation from the R state and bimolecular ligand recombination, thus the microscopic rate constants for the R → T transition and CO recombination are convoluted together in τ_4. Finally, processes 5 and 6 correspond to fast and slow bimolecular recombination of CO to the R and T state conformations of the protein, respectively.

Spectral evolutions (b-spectra) associated with each of the six time constants resulting from global fitting of the PEG-free data are shown in Fig. 2 *A*. As expected, the spectral signatures associated with both the geminate and the bimolecular CO rebinding events (processes 1, 2, 5, and

TABLE 1 Time constants and percent amplitudes as a function of [PEG-200], obtained from fitting of HbCO absorption data to six exponential relaxations

	τ (Amplitude)					
Percent*	**1** (ns)	**2** (ns)	**3** (μs)	**4** (μs)	**5** (μs)	**6** (ms)
0	22 ± 3	109 ± 16	2.1 ± 0.7	44 ± 12	183 ± 18	3.9 ± 0.3
	(31 ± 4)	(20 ± 3)	(2 ± 1)	(11 ± 3)	(27 ± 2)	(10 ± 1)
10	25 ± 3	111 ± 10	1.6 ± 0.5	51 ± 4	199 ± 11	4.6 ± 0.9
	(29 ± 2)	(21 ± 2)	(3 ± 1)	(12 ± 2)	(26 ± 1)	(8 ± 1)
20	28 ± 4	139 ± 18	2.8 ± 1.2	60 ± 10	213 ± 23	4.0 ± 1.0
	(30 ± 3)	(20 ± 3)	(2 ± 1)	(15 ± 2)	(26 ± 3)	(5 ± 1)
30	31 ± 6	147 ± 13	2.9 ± 0.3	64 ± 6	228 ± 31	4.0 ± 0.9
	(31 ± 2)	(21 ± 2)	(2 ± 1)	(18 ± 1)	(25 ± 1)	(4 ± 1)

pH 7.3, 20°C.
*Percent by weight.

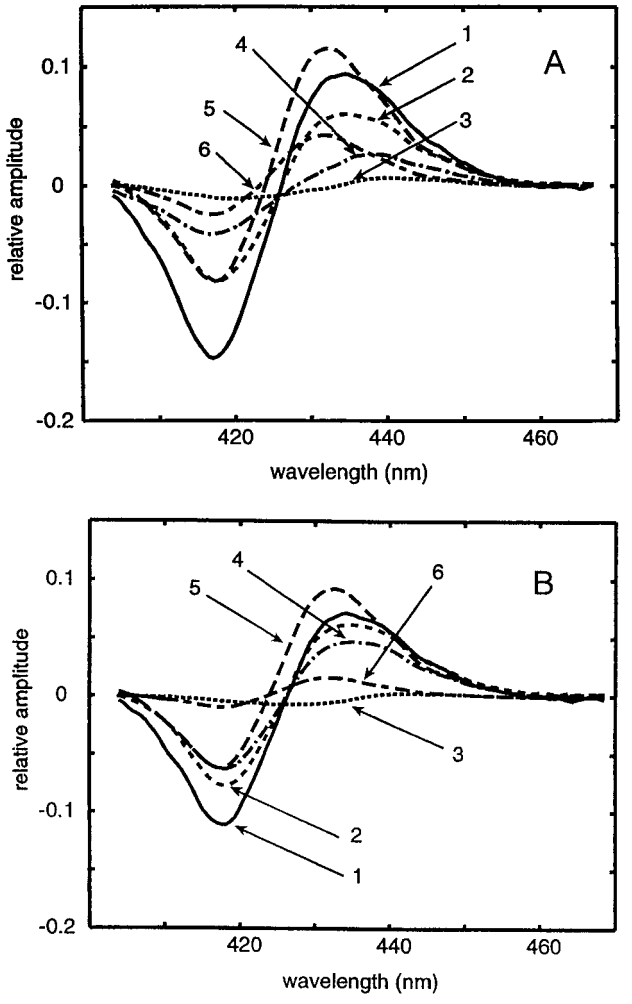

FIGURE 2 Soret band absorbance changes (b-spectra) associated with the time constants reported in Table 1. Relaxations: 1 (—), 2 (- -), 3 (· · ·), 4 (– · –), 5 (– –), and 6 (– - –). (*A*) PEG-free; (*B*) 30% PEG-200.

6) resemble the equilibrium deoxyHb-HbCO difference spectrum (Hofrichter et al., 1983; Esquerra et al., 2000). In contrast, the b-spectrum associated with process 3, although very small in amplitude, is very similar in shape to the static T-R spectral difference spectrum reported by Perutz et al. (1974), consistent with the other evidence for quaternary structural changes on this time scale mentioned above. The b-spectrum associated with the $R_0 \rightarrow T_0$ structural transformation (process 4) is a mixture of the deoxyHb-HbCO difference spectrum and the T-R difference spectrum, consistent with the branching nature of this process, also mentioned above. More discussion of the assignments used here for the time constants and their spectral signatures can be found in Goldbeck et al. (1996) and in references cited therein.

The time constants and amplitudes listed as a function of PEG-200 concentration in Table 1 show that the polymer appears to broadly affect most processes. The two time constants associated with geminate recombinations, τ_1 and τ_2, both increase by 40 (±20)% on going from 0 to 30% PEG (the percent changes reported here and their uncertainties were calculated from linear regression analyses), without significant amplitude changes. The time constant for the fast phase of the allosteric transition, τ_3, also appears to increase, by 70%, but the uncertainty of this change, ±60%, is very high because of the small amplitude of the process. However, the increase in the time constant associated with the larger amplitude phase of the $R_0 \rightarrow T_0$ quaternary transition, τ_4, is clearly significant, 50 (±20)%. This change is accompanied by an increase of 70 (±30)% in spectral amplitude as well. The time constant for bimolecular CO-rebinding to $R_{(1–3)}$-state hemes, τ_5, shows a modest increase, 25 (±5)%, and no significant change in amplitude. However, the time constant for millisecond CO rebinding to T state hemes is not affected by PEG, but its amplitude decreases sharply, 64 (±7)%.

Changes in the shapes and integrated intensities (the latter are reflected in the amplitude changes reported above) of the Soret b-spectra as a function of increasing polymer concentration are shown in Fig. 2 *B*. The minimum of the negative lobe of the b-spectrum associated with process 2 shifts by ~2 nm to shorter wavelengths. A shoulder shifts the deoxy peak maximum from 440 nm to 434 nm, and the negative lobe increases in intensity by ~20%, providing an R state CO-rebinding feature to the b-spectrum associated with the $R_0 \rightarrow T_0$ transition (process 4). Changes in the relative magnitudes of extrema within the rebinding spectra are also observed in the presence of PEG. The intensity of the positive lobes of the b-spectra associated with bimolecular CO rebinding to $R_{(1–3)}$-state hemes and with geminate CO recombination to the prompt photoproduct both decrease by ~35%, whereas the negative lobes decrease in intensity by ~55% and 20%, respectively. The positive and negative lobes of the b-spectrum associated with CO rebinding to T-state hemes decrease in intensity by ~75% and 30%, respectively.

The first basis spectrum, U_1, which corresponds primarily to the deoxy-carboxy difference spectrum, and its corresponding time course, V_1, which largely reflects the course of CO rebinding (Goldbeck et al., 1996), are shown in Fig. 3. The intensity of both SVD components are diminished by the presence of 30% PEG-200. This is particularly evident in U_1 (*panel A*) near the 434-nm absorption peak of the deoxyHb phototransient and in V_1 (*panel B*) during mid to late milliseconds, the time during which CO rebinds from the solvent to T-state hemes. This effect is also manifested by the PEG-induced attenuation of the Soret time-resolved absorption difference spectra recorded during the millisecond time regime (Fig. 1 *B*).

Increasing the concentration of PEG-200 from 0 to 30% changed the pH of the phosphate buffer from 7.3 to 7.75 (±0.1). Therefore, to determine how much of the observed PEG-induced kinetic perturbations were due to accompany-

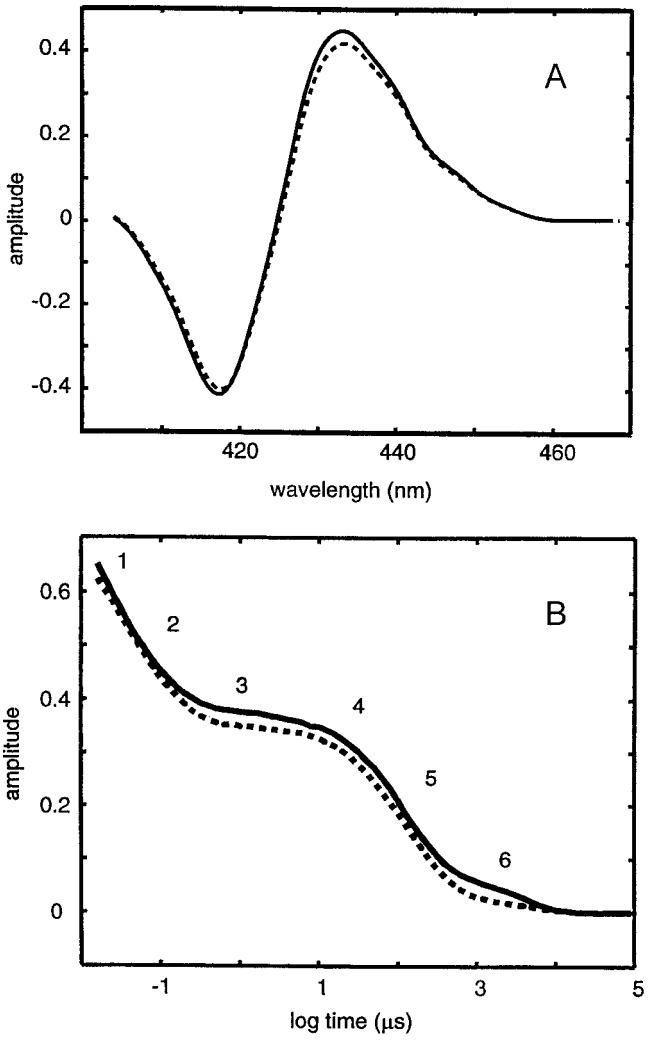

FIGURE 3 First SVD component of the data shown in Fig. 1. (*A*) Basis spectra (U_1) for PEG-free (*solid line*) and 30% PEG-200 (*dashed line*) solutions. (*B*) Amplitude time courses (V_1), legend as in (*A*).

ing changes in solution pH, time-resolved absorption difference spectra were recorded for HbCO in PEG-free buffer solutions made more alkaline with the dibasic component (HPO_4^{2-}) of the phosphate buffer. The results of a six-exponential fitting analysis of Soret time-resolved absorption difference spectra measured in PEG-free solutions at pH 7.3 are compared with kinetic results obtained in PEG-free solutions at pH 7.6, 7.75, and 7.9 in Table 2. The time constants for processes 1–4 did not change significantly over this pH range. The time constants for R- and T-state recombination decreased by 23 (±8) and 38 (±11)%, respectively. The amplitudes for all processes were largely unchanged, except those for processes 2 and 6. The amplitude for the second geminate process increased modestly, 30 (±10)%, whereas the amplitude for T-state ligand recombination dropped more sharply, 50 (±10)%.

TABLE 3 Microscopic $R_0 \rightarrow T_0$ rate constants and parameters describing cosolute conditions

% PEG	Osmolality	pH	η (cP)	$k_{R_0 \rightarrow T_0}$ (s^{-1})
0	0.21	7.3	1.0	10,600 ± 1800
0	0.22	7.6	1.0	9500 ± 2000
0	0.22	7.75	1.0	6900 ± 1600
0	0.22	7.9	1.0	5300 ± 1500
10	0.55	7.45	1.8	7100 ± 1500
20	1.24	7.6	2.8	3800 ± 1000
30	2.10	7.75	3.9	2700 ± 800

20°C.

The values for $k_{R_0 \rightarrow T_0}$, the microscopic R → T rate constant, shown in Table 3 were estimated from the time constant and amplitude values in Tables 1 and 2 using the relation:

$$A_6 = 4A_0R_0k_{R_0 \rightarrow T_0}/(k_{R_0 \rightarrow T_0} + 4k_{R+CO}) + 3A_0R_1k_{R_1 \rightarrow T_1}/(k_{R_1 \rightarrow T_1} + 3k_{R+CO}) \quad (2)$$

where A_6 is the spectral amplitude for process 6, $4A_0$ is the total amplitude for bimolecular ligand recombination, R_0 and R_1 are the fractional populations of deliganded and singly liganded tetramers produced by photolysis, respectively, and k_{R+CO}, the pseudo-first-order rate constant for

TABLE 2 Time constants and percent amplitudes as a function of pH, obtained from fitting of HbCO absorption data to six exponential relaxations

	τ (Amplitude)					
pH	**1** (ns)	**2** (ns)	**3** (μs)	**4** (μs)	**5** (μs)	**6** (ms)
7.3	22 ± 3	109 ± 16	2.1 ± 0.7	44 ± 12	183 ± 18	3.9 ± 0.3
	(31 ± 4)	(20 ± 3)	(2 ± 1)	(11 ± 3)	(27 ± 2)	(10 ± 1)
7.6	26 ± 3.4	93 ± 7.3	0.8 ± 0.4	48 ± 0.2	150 ± 11	2.8 ± 0.4
	(29 ± 1)	(20 ± 1)	(3 ± 1)	(14 ± 1)	(27 ± 1)	(8 ± 1)
7.75	22 ± 0.7	98 ± 1.1	1.0 ± 0.3	42 ± 0.1	142 ± 8	2.7 ± 0.4
	(31 ± 3)	(21 ± 1)	(2 ± 1)	(11 ± 1)	(29 ± 1)	(6 ± 1)
7.9	17 ± 1.5	87 ± 6	1.2 ± 0.2	43 ± 4	141 ± 7	2.4 ± 0.2
	(29 ± 1)	(25 ± 1)	(2 ± 1)	(12 ± 1)	(26 ± 1)	(5 ± 1)

20°C.

R-state ligand recombination, is given by τ_5^{-1}. The statistical factors in front of k_{R+CO} reflect the number of hemes available for ligand binding in an R_0 or R_1 tetramer. The value of A_0 was calculated from $A_0 = (1 - d)(f A_4 + A_5 + A_6)/4$, where the term $d = 0.10$ accounts for the fraction of hemes that will be present in the form of dissociated dimers at the concentration of hemoglobin used in these studies, and therefore not able to undergo the R → T transition, and the factor $f = 0.80$ corrects A_4 for the contribution ($\sim 0.2A_0$) expected from the $R_0 \rightarrow T_0$ transition spectral difference. The latter contribution was estimated roughly by dividing the peak molar extinction difference between R_0 and T_0, $1.7 \times 10^4\ M^{-1}\ cm^{-1}$ (Perutz et al., 1974), by a quarter of the peak molar extinction for the deoxy-carboxy difference spectrum ($\sim 10^6\ M^{-1}\ cm^{-1}$), and multiplying by R_0 and the $R_0 \rightarrow T_0$ branching ratio, ~0.4. R_0 and R_1 were calculated from the prompt photolysis yield, $\Phi = 90\%$, using a binomial statistical distribution. (Note that Eq. 2 assumes that the R → T contribution to A_6 originating from the R_2 and R_3 photolysis populations can be neglected because the corresponding T → R back reactions are expected to be rapid, allowing those populations to efficiently recombine with ligand on the τ_5 time scale. In any event, R_2 and R_3 are expected to be small under the photolysis conditions used.) Equation 2 was simplified by setting $k_{R_1 \rightarrow T_1} = c\ k_{R_0 \rightarrow T_0}$, where the value measured by Sawicki and Gibson (1976), $c = 0.4$, was used. [A similar value for c is also obtained if one considers the linear free energy relationship between $k_{R_i \rightarrow T_i}$ and L_i, the $R_i \leftrightarrow T_i$ equilibrium constant, reported by Eaton et al. (1991) and the variation of L_i with ligation.] The quadratic equation obtained by substituting this expression for $k_{R_1 \rightarrow T_1}$ into Eq. 2 was solved for $k_{R_0 \rightarrow T_0}$ at each set of solution conditions in Table 3. Similar results (not shown) were also obtained from an independent method for estimating $k_{R_0 \rightarrow T_0}$ using the A_6 and τ_4 values in Tables 1 and 2. This method used the relation

$$k_{R_0 \rightarrow T_0} = \tau_4^{-1} A_6 (4A_0 R_0)^{-1} \quad (3)$$

which assumes that both $A_6\ (4A_0\ R_0)^{-1}$ and $\tau_4\ k_{R_0 \rightarrow T_0}$ are equal to the microscopic $R_0 \rightarrow T_0$ yield. Although the two approaches gave similar results, the estimates from Eq. 2 were judged to be more accurate because the correction for R_1 photolysis product could be incorporated more easily than was possible with Eq. 3.

DISCUSSION

In determining the effect of osmolytes such as PEG on relaxation rates in hemoglobin, it is important to consider all of the environmental properties through which cosolutes can affect relaxation kinetics. The solution pH and viscosity, in particular, are both known to affect heme-pocket dynamics after photolysis. Low pH is known to speed heme-pocket tertiary relaxation rates in hemoglobin (Scott and Friedman, 1984) and to speed the R → T transition (Sawicki and Gibson, 1976). More specifically, the pH dependence of $k_{R_0 \rightarrow T_0}$ can be described using the Bohr effect, the variation of $L_0 = [T_0]/[R_0]$ due to proton binding ($L_0 \propto [H^+]^n$, where the number of Bohr protons $n = 2$), in conjunction with the following linear free energy relation between ΔG, the $T_0 - R_0$ free energy difference, and $\Delta G^{\ddagger}$, the $R_0 \rightarrow T_0$ activation free energy change (Szabo, 1978),

$$\Delta G^{\ddagger} = \alpha \Delta G + \text{constant} \quad (4)$$

where the value $\alpha = 0.17 \pm 0.02$ was reported by Eaton et al. (1991).

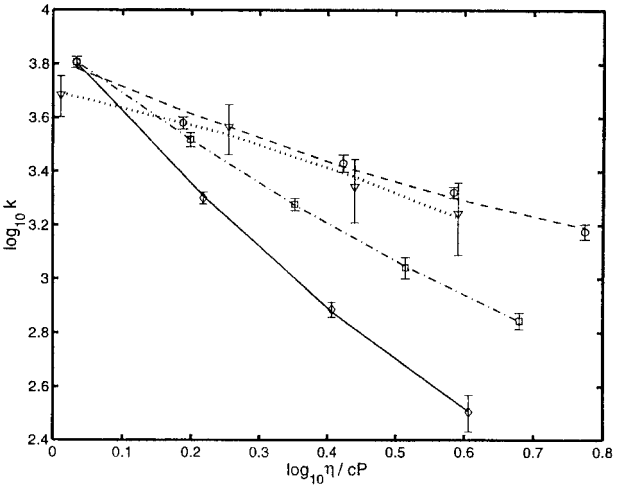

FIGURE 4 Log-log plot of $k_{R_0 \rightarrow T_0}$ versus viscosity for HbCO with various cosolute solutions (pH 8.3): PEG-200, 0.1 M phosphate (*triangle*, · · ·); sucrose, 0.1 M borate (*open circle*, – – –); glycerol, 0.1 M borate (*open square*, · – · – · –); and ethylene glycol, 0.1 M borate (*open diamond*, —). PEG-200 values were taken from Table 3 and pH-adjusted to 8.3, as described in text. The values of k and error bars for sucrose, glycerol, and ethylene glycol are taken from Sawicki and Khaleque (1983). Lines are polynomial fits intended only to connect points for a cosolute.

Solvent viscosity appears to slow heme-pocket relaxation kinetics broadly over a time regime from tens of nanoseconds to milliseconds after photolysis of HbCO (Findsen et al., 1988). Sawicki and Khaleque (1983) examined the effect of viscosity on $k_{R_0 \rightarrow T_0}$, in particular. They found a decrease in the allosteric rate constant as a function of increasing viscosity associated with the addition of various cosolutes. However, it is significant that they observed that the effectiveness of viscosity in slowing the transition seemed to depend strongly on the chemical identity of the cosolute, the effectiveness being greatest for the smallest cosolute studied, ethylene glycol, and least for the largest, sucrose (see Fig. 4). They suggested that the macroscopic and microscopic viscosities produced by a given cosolute might differ, possibly explaining the discrepant kinetic effects of the cosolutes when tabulated versus their macroscopic viscosities. Similarly, Findsen et al. (1988) noted that the change in heme-pocket relaxation kinetics they observed

with the addition of glycerol as cosolute seemed larger than expected simply from a dependence of side chain diffusional motion on viscosity, an observation they interpreted as evidence for larger scale protein motions accompanying heme-pocket relaxation. These observations of an enhanced viscosity effect for small cosolutes suggest to us that solvent properties independent of viscosity may also be important in explaining the kinetic effects of cosolutes. We evaluate below evidence for the proposal that the solvent activity is one such property that cannot be neglected in cosolute kinetic studies of protein allostery.

The effect of pH on relaxation rates noted above is not generally apparent in the values for the time constants listed in Table 2. For processes 1–3 this is probably because the signal-to-noise ratios are not high enough to detect the modest changes expected for these processes over this pH range. However, both the R- and T-state bimolecular recombination processes are significantly faster at higher pH. Although the time constant most closely identified with allosteric relaxation, τ_4, is also relatively unchanged, this is not inconsistent with the drop in $k_{R_0 \rightarrow T_0}$ for the high pH values shown in Table 3. The latter change stems from the 50% drop in amplitude for T-state production, A_6, which indicates that the R $\rightarrow$ T branching yield, and thus by implication $k_{R_0 \rightarrow T_0}$, decreases. If we adopt the simplifying assumption that $\tau_4 = (k_{R_0 \rightarrow T_0} + 4k_{R+CO})^{-1}$ (neglecting the contribution of the $R_1 \rightarrow T_1$ transition to the kinetics on this time scale and the likelihood that α,β-chain kinetic heterogeneity also affects τ_4 and τ_5), we see that the decrease in $k_{R_0 \rightarrow T_0}$ calculated in Table 3 from the trend in A_6 is offset by the increase observed in k_{R+CO} (τ_5^{-1}) such that τ_4 remains relatively independent of pH. As will be shown below, the pH variation in the $k_{R_0 \rightarrow T_0}$ values displayed in Table 3 is consistent with the linear free energy relation mentioned above.

Much of the broad slowing of time constants observed in Table 1 with increasing PEG concentration (an effect that is enhanced when we consider that the pH effect of PEG tends to shorten some of those time constants) may be due to viscosity (η values are shown in Table 3). For instance, the increases in time constants for processes 1–4 may be attributed at least in part to the effect of increasing viscosity on structural relaxation rates noted above. On this basis, some effect of viscosity on the geminate recombination processes 1 and 2 can be expected from slowing of a tertiary heme-pocket relaxation that is thought to lower the activation barrier for geminate recombination (Findsen et al., 1988).

Only a small increase in time constant was observed for R-state bimolecular recombination, process 5, and a similar insensitivity to viscosity was observed previously for bimolecular recombination by Sawicki and Khaleque (1983). This insensitivity might be unexpected given the much larger increase naively expected for a diffusive bimolecular process. Diffusion-controlled bimolecular rate constants are inversely proportional to viscosity, which varies by a factor of 4 over the PEG concentrations represented in Table 1. However, bimolecular CO recombination in heme proteins is typically not diffusion-controlled because the rate-limiting step is internal to the protein, as shown for myoglobin by McKinnie and Olson (1981). Those authors point out that the bimolecular rate constant for CO binding can actually increase in viscous solutions. They found that the key factor in explaining bimolecular rate constants in the presence of cosolutes was the effect of cosolute on the chemical potential of the ligand, i.e., ligand solubility. We report pseudo-first-order time constants, which depend on the product of the ligand concentration and the second order rate constant. Because McKinnie and Olson found that the second-order rate constant was inversely proportional to the ligand solubility, any changes in these factors induced by cosolute are expected to cancel in the pseudo-first-order rate constants. Another way of saying this is that in the limit that bimolecular diffusion within the solution is much more rapid than all other steps in the ligand combination reaction, then a steady-state ratio will be established between the external CO pressure and the concentration of those CO molecules that leave the solution to associate with the protein matrix. This ratio is determined by the chemical potentials for CO in the gas phase and CO associated with the protein, and is independent of the solution properties. If instead of instantaneous communication we more realistically assume a finite diffusion-controlled bimolecular rate constant of 10^9–10^{10} M^{-1} s^{-1} for a 1 mM CO solution (dissolved CO present in excess over protein), then we can estimate that there will be 100–1000 collisions between CO molecules and a given protein molecule during the roughly 10^{-4} s required for CO to recombine with heme iron in the R-state tetramer. Because this collision number estimate will vary inversely with solution viscosity, such a large number assures that the bimolecular rebinding kinetics in cosolute solutions with viscosities $<\sim$10 cP will remain close to that predicted by an idealized scenario that assumes instantaneous communication between CO in the gas phase and CO interacting with the protein, a scenario that predicts that the observed time constants will be independent of solvent properties such as viscosity and CO solubility. The small but finite effect of viscosity observed in the R-state recombination process appears to be absent in the T-state process, suggesting that T-state recombination, being slower, is even closer to this ideal scenario than R-state recombination.

Although viscosity is widely thought to modulate structural relaxation rates in hemoglobin, previous viscosity studies (Findsen et al., 1988; Sawicki and Khaleque, 1983) supporting this conclusion have not considered or controlled for solvent activity. The data presented for hemoglobin processes 1–4 in PEG cosolute (Table 1) can be equally well modeled on the basis of viscosity or osmotic effects (results not shown) and thus are not decisive on this point. However, it is useful to plot the $k_{R_0 \rightarrow T_0}$ values obtained for PEG-200 in Table 3 together with the values reported by

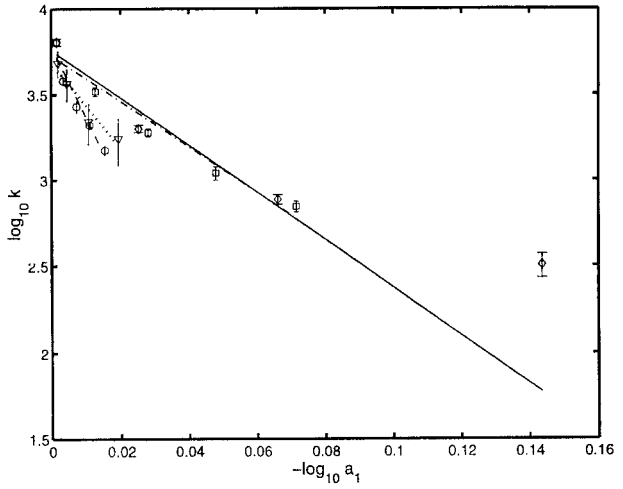

FIGURE 5 Log-log plot of $k_{R_0 \rightarrow T_0}$ versus a_1, the activity of water, for HbCO with various cosolutes (pH 8.3). Labels, conditions, and data sources as described in Fig. 4 legend. The lines represent linear regression fits to the data points. The highest weight fraction data point (0.49) was omitted from the regression fit for the ethylene glycol data (see text).

Sawicki and Khaleque (1983) for three other viscous cosolutes, sucrose, glycerol, and ethylene glycol, displaying them either as a function of viscosity, η, as shown in Fig. 4, or as a function of water activity, a_1, as shown in Fig. 5. [Water activities for the aqueous sucrose, glycerol, and ethylene glycol solutions were calculated from published tables of osmolality (Osm) versus cosolvent weight fraction (Weast, 1972) using the relation Osm $= -55.5 \ln a_1$. The water activities of the PEG-200 solutions were estimated from the empirical relation $a_1 = x_1 - 0.02$ M $(1 - x_1)^2$, where M is the cosolvent molecular weight and x_1 is the mole fraction of water. This expression reproduced water activities calculated from osmolality tables for the other three cosolvents to within $\pm 2\%$ over the cosolvent weight fraction range 0–0.4. The nonideality correction represented by the second term was $<1\%$ for the PEG solutions relative to an ideal (Raoult's Law) solution in which $a_1 = x_1$. The PEG kinetic constants from Table 3 were adjusted to pH 8.3 in Figs. 4 and 5 for comparison with the results of Sawicki and Khaleque using the linear free energy expression described above.] Although the correlation between rate constants and solvent properties in neither plot is definitive, plotting versus solvent activity does seem to provide a less scattered representation of the data obtained for all of the cosolutes. This is particularly evident in Fig. 5 for the smallest cosolutes, ethylene glycol and glycerol, which have the greatest effect on solvent activity for a given value of viscosity (although the point corresponding to the smallest rate constant reported for ethylene glycol appears to be an outlier). Taken together, the lack of satisfactory correlations in Figs. 4 and 5 suggest that both viscosity and osmotic effects are present and that both must be considered when modeling solvent effects on R $\rightarrow$ T transition rates.

The effect of viscosity on thermally activated rate processes was first considered by Kramers (1940), but it was not widely studied by chemists until the 1970s (Gegiou et al., 1968), and it remains an active area of research (Pollak, 1996). Kramers considered the effect of a mass weighted frictional coefficient, β, on the rate of passage from reactants to products along a one-dimensional reaction coordinate and found solutions valid in two limits, low and high friction. In the high-friction limit applicable to liquid phase reactions, the reaction rate is limited by spatial diffusion along the reaction coordinate and is asymptotically inversely proportional to β. Because the value of β cannot usually be measured directly, the friction encountered along the reaction coordinate is typically assumed to be proportional to the more easily measured quantity η, the shear viscosity of the bulk liquid. With this assumption, one arrives at the viscosity dependence of thermally activated rate constants that is usually associated with the Kramers theory:

$$k \propto \eta^{-1} \tag{5}$$

Observations of the viscosity dependence of activated rate processes occurring within proteins frequently deviate from the simple Kramers behavior of Eq. 5 (Beece et al., 1980; Lavalette and Tetreau, 1988; Rosenberg et al., 1989). The non-Kramers behavior observed in proteins is often described empirically by introducing a parameter ν, $0 < \nu < 1$, into the viscosity dependence,

$$k \propto \eta^{-\nu} \tag{6}$$

a procedure that has been rationalized by several theoretical treatments (Gavish, 1980; Doster, 1983; Schlitter, 1988; Zwanzig, 1992; Okada, 2000). However, the value of ν observed for a rate process may depend on the nature of the cosolute used to increase the solution viscosity. Yedgar et al. (1995) reported that the value of ν measured for the thermally activated escape of ligand photodissociated from hemerythrin appears to be a function of the molecular weight of the cosolute, such that the observed viscosity dependence nearly vanishes as the molecular weight of the cosolute becomes very large ($\geq 10^5$). A similar effect was observed for the diffusion of tritium oxide in aqueous viscous cosolutes, diffusion becoming nearly independent of the viscosity of the bulk solution ($\nu < 0.1$) as the cosolute molecular weight exceeded $\sim 10^5$ (Barshtein et al., 1995). The latter two observations suggest that microscopic inhomogeneities in the solution viscosity may become important when cosolutes are very large, i.e., the microviscosity in regions where individual rate process events occur may effectively be closer to that of pure water than to the macroscopic viscosity (Barshtein et al., 1995). Yedgar et al. (1995) derived an empirical expression for estimating the value of ν for a cosolute of molecular weight M,

$$\nu(\mathrm{M}) = 1.52\ \mathrm{M}^{-0.23} \tag{7}$$

based on their hemerythrin measurements in ethylene glycol, glycerol, glucose, sucrose, and dextran polymer (M = 1,600–500,000) cosolutes.

An alternative expression for the non-Kramers effect of viscosity on protein rate processes,

$$k \propto (\sigma + \eta)^{-1} \tag{8}$$

was introduced by Ansari et al. (1992) in a study of conformation relaxation in myoglobin. This expression introduces the parameter σ, which is attributed to internal protein viscosity. Briefly, those authors envisioned hindered intrachain motion within the protein as providing a friction that adds to the friction from solvent molecules at the protein surface in resisting relaxation of protein structure after a perturbation such as heme ligand photodissociation. In their model, the ratio of σ to η is equal to $\gamma\zeta_p/(1 - \gamma)\zeta_s$, where γ is the fraction of protein atoms involved in conformational change that are not in contact with solvent, and $\zeta_{p,s}$ is a friction constant for motion in the protein (p) or solvent (s). Those workers measured a σ value of 4.1 $\pm$ 1.3 cP for myoglobin averaged over the temperature range -5 to 35°C.

The treatments of solvent viscosity effects in proteins described above rely on the introduction of an empirical fitting parameter, ν or σ, that is usually assumed to be protein-dependent, although Yedgar et al. (1995) proposed that ν values depend strongly on the nature of the viscous cosolvent. The physical interpretation of σ as an internal protein viscosity advanced by Ansari et al. (1992) could lead to inferences about relative γ values from viscosity data for rate processes in homologous proteins if one assumes that homologous proteins have identical ζ_p values, although experimental measurements of values for ζ_p do not appear to be available to evaluate this assumption. Further measurements of σ values for other proteins are needed to test their interpretation. The more widely applied parameter ν is often interpreted as a measure of the strength of coupling between solvent frictional forces and the reaction coordinate friction coefficient, with $\nu = 1$ reflecting strong coupling. In this sense, it plays a role similar to that of γ, with $\nu = 1$ corresponding to $\gamma = 0$ and $\nu = 0$ corresponding to $\gamma = 1$. However, most reported ν values fall in a relatively narrow range well between these limits, 0.4–0.6 (Yedgar et al., 1995). In the latter regard, the experiments of Yedgar et al. (1995) suggest that more fundamental factors, such as the microscopically inhomogeneous nature of mixed solvents, may actually underlie at least some of the non-Kramers viscosity effects typically attributed to protein forces. That proposal would explain the narrow range of ν values observed for the variety of proteins examined as being a consequence of the narrow range of molecular weights presented by the most commonly used viscous cosolutes. It seems reasonable to suppose that both internal protein forces and microscopic solvent inhomogeneity can affect the coupling of bulk solvent viscosity to the coefficient of friction along the protein reaction coordinate, but the relative importance of these effects and their functional dependences on solvent and protein parameters remain open questions. Given the lack of consensus in the literature on how to treat viscosity effects in proteins, each of the approaches described above was considered in turn in the analysis of kinetic data discussed below.

In considering the effect of solvent activity on rate constants for reactions that change the number N_w of water molecules solvating a protein, we consider first its effect on the equilibrium constant, K_{eq}. Because it is possible that cosolute molecules used to lower water activity may also replace water molecules in the protein's solvation layer, we start with an expression valid in the presence of such protein-cosolute interactions

$$(\partial \ln K_{eq}/\partial \ln a_1)_{a_x} = -\Delta\Gamma_{\mu_3} \tag{9}$$

where the subscript on the partial derivative indicates that the activities of reactants and products are held constant (as well as temperature and pressure), the protein activity (a_2 in Scatchard notation) is assumed to be vanishingly small, and $\Delta\Gamma_{\mu_3}$ is the stoichiometrically weighted difference in solute-protein preferential interaction coefficients (Courtenay et al., 2000). A Γ_{μ_3} coefficient characterizes the interaction of a cosolute with each reactant or product in the reaction, where

$$\Gamma_{\mu_3} \equiv (\partial m_3/\partial m_2)_{T,P,\mu_3} \tag{10}$$

is the variation in cosolute molality with protein molality at constant T, P, and cosolute chemical potential. Equation 9 can be rewritten in the local-bulk domain model (the local domain is essentially the solvation monolayer) of Courtenay et al. (2000) as

$$(\partial \ln K_{eq}/\partial \ln a_1)_{a_x} = \Delta[N_w(1 - K_P)] \tag{11}$$

where K_P is the cosolute local-bulk partition coefficient defined by

$$K_P \equiv \frac{(N_3/N_1)}{(m_3/m_1)} \tag{12}$$

in which N_1 and N_3 are, respectively, the number of water and cosolute molecules in the local domain, and N_w is the number of water molecules solvating the protein in the absence of cosolute, i.e., $\lim_{m_3 \to 0} N_1 = N_w$. Thus, $K_P = 0$ for a perfectly excluded cosolute, $0 < K_P < 1$ for an imperfectly excluded cosolute, $K_p = 1$ for a randomly distributed cosolute (water and cosolute composition of the local domain identical to that of the bulk solution), and $K_P > 1$ for a cosolute that interacts preferentially with the protein.

For a perfectly excluded cosolute, Eq. 11 reduces to

$$(\partial \ln K_{eq}/\partial \ln a_1)_{a_x} = \Delta N_w \tag{13}$$

where ΔN_w is the change in the number of water molecules solvating the protein. This approximation, discussed further below, is used frequently in studying osmotic stress effects in hemoglobin (Parsegian et al., 1995). Equation 13 can be understood heuristically by dropping for a moment the convention followed elsewhere in this work that solvent molecules not appear explicitly in reaction stoichiometries and writing, for example, Reactant $\cdot (H_2O)_{N_R} + \Delta N_w$ H_2O = Product $\cdot (H_2O)_{N_P}$, where $N_{R,P}$ is the total number of waters solvating reactant or product and $\Delta N_w = N_P - N_R$. The overall equilibrium constant for this reaction, K_{all}, and the conventional equilibrium constant, K_{eq}, are related in terms of activities by $K_{all} = a_{product} a_{reactant}^{-1} a_1^{-\Delta N_w} = K_{eq}$ $a_1^{-\Delta N_w}$, or $K_{eq} = K_{all}\ a_1^{\Delta N_w}$, from which Eq. 13 follows directly (for variations in a_1 induced by perfectly excluded cosolutes).

Eq. 11 can be rewritten, using $RT \ln K_{eq} = -\Delta G_o$ (R is the universal gas constant), as

$$(\partial\ \Delta G_o/\partial\ \ln\ a_1)_{a_x} = -RT\Delta[N_w(1 - K_P)] \qquad (14)$$

an expression that can be used to adjust the standard free energy change of the reaction for changes in water activity, the size of the correction depending on the changes in N_w and K_P. Equations 11 and 14 predict that equilibria between protein conformations requiring equal numbers of solvating waters are independent of water activity, as are measurements using a randomly distributed cosolute ($K_P = 1$). For equilibria observed to depend on water activity, however, measurements of K_{eq} vs. a_1 ("osmotic stress" measurements) can be used to deduce a value for ΔN_w with the aid of Eq. 11 and independent knowledge of (or assumptions about) K_P.

A transition state complex is envisioned as being in equilibrium with reactants in transition state theory. The rate constant for a reaction is then proportional to the transition state complex equilibrium constant, $K^{\ddagger}$

$$k = CK^{\ddagger} \qquad (15)$$

where C is independent of the reactant and transition state free energies. By analogy with Eq. 9, we can write the following expression for the dependence of the equilibrium between reactants and the transition state complex on water activity

$$(\partial\ \ln\ K^{\ddagger}/\partial\ \ln\ a_1)_{a_x^{\ddagger}} = \Delta[N_w(1 - K_P)]^{\ddagger} \qquad (16)$$

where the right-hand side is the change in the quantity $N_w(1 - K_P)$ in the transition state relative to the reacting state and the partial derivative is taken with respect to constant reactant and transition state complex activities. For $K_P = 0$, the right-hand side of Eq. 16 reduces to $\Delta N_w^{\ddagger}$, the number of additional water molecules required to solvate the transition state. As for Eq. 11, Eq. 16 is rewritten as

$$(\partial\ \Delta G_o^{\ddagger}/\partial\ \ln\ a_1)_{a_x^{\ddagger}} = -RT\Delta[N_w(1 - K_P)]^{\ddagger} \qquad (17)$$

which can be integrated over limits representing pure solvent and a mixed solvent-cosolvent solution of water activity a_1 (neglecting the small effect of protein concentration on a_1)

$$\int_{a_1'=1}^{a_1'=a_1} d\Delta G_o^{\ddagger} = -RT\Delta[N_w(1 - K_P)]^{\ddagger} \int_0^{\ln a_1} \mathrm{d}\ \ln\ a_1' \qquad (18)$$

to give the explicit dependence of the activation free energy on water activity

$$\Delta G_o^{\ddagger}(a_1) = \Delta G_o^{\ddagger}(a_1 = 1) - RT\Delta[N_w(1 - K_P)]^{\ddagger}\ \ln\ a_1 \qquad (19)$$

Recasting Eq. 19 in terms of the a_1 dependence of the activation equilibrium constant gives

$$K^{\ddagger}(a_1) = K^{\ddagger}(a_1 = 1) a_1^{\Delta[N_w(1-K_P)]^{\ddagger}} \qquad (20)$$

Combining Eqs. 15 and 20 yields

$$k \propto a_1^{\Delta[N_w(1-K_P)]^{\ddagger}} = a_1^{\Delta N_{obs}^{\ddagger}} \qquad (21)$$

for the functional dependence of the reaction rate constant on water activity in the presence of imperfectly excluded cosolutes, where we have defined $\Delta N_{obs}^{\ddagger} \equiv \Delta[N_w(1 - K_P)]^{\ddagger}$. If we assume that K_P is unchanged by the reaction, then $\Delta N_{obs}^{\ddagger} = \Delta N_w^{\ddagger}(1 - K_P)$. This expression says that the observed activity-dependence exponent will be reduced in magnitude by a factor $(1 - K_P)$ from the true change in hydration number for an imperfectly excluded cosolute (and inverted in sign for cosolutes that interact preferentially with the protein).

We combined the dependence of allosteric rate constants on water activity derived from transition state theory in Eq. 21 with the expressions for non-Kramers dependence on solution viscosity presented in Eqs. 6–8 to obtain several expressions for the allosteric rate constant in hemoglobin, $k_{R_0 \rightarrow T_0}$, each of which was used to analyze the kinetic data considered here. Consider first the following expression incorporating the effects of the viscosity dependence in Eq. 8, solvent activity, and pH

$$k_{R_0 \rightarrow T_0} = C_0(\sigma + \eta)^{-1} a_1^{\Delta N_{obs}^{\ddagger}} ([H^+]/[H^+]_0)^{2\alpha} \qquad (22)$$

where C_0 is the rate constant at $\eta = 1$, $\sigma = 0$, $a_1 = 1$, and $[H^+] = [H^+]_0$; σ and η are the internal protein viscosity discussed above and the bulk solvent viscosity, both relative to the viscosity of water, $\eta_o = 1$ cP; $\Delta N_{obs}^{\ddagger}$ is the observed number of additional water molecules required to solvate the transition state; α is the free energy proportionality factor; and $[H^+]_0 = 10^{-7.3}$ M. The pH expression, $([H^+]/[H^+]_0)^{2\alpha}$, combines the Bohr effect on L_0 with the linear free energy relation for $k_{R_0 \rightarrow T_0}$ described above (Eaton et al., 1991). The allosteric rate constants in Table 3, along

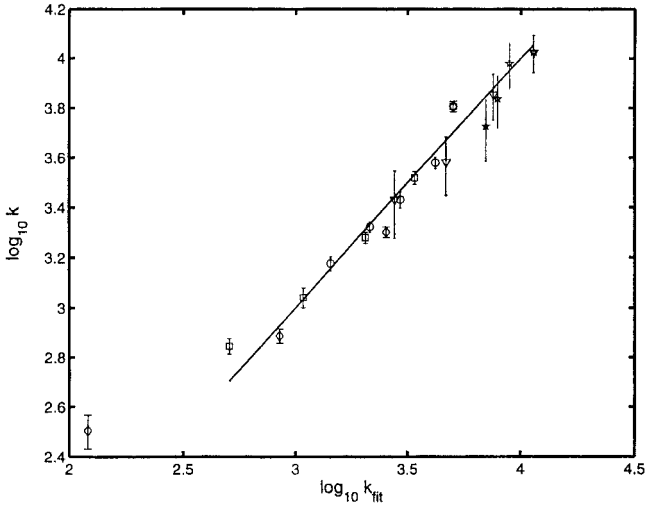

FIGURE 6 Log-log plot of $k_{R_0 \rightarrow T_0}$ calculated from fit to Eq. 22 versus experimental values for HbCO with various cosolutes, using the corresponding fitting parameters in Table 4. PEG-200, 0.1 M phosphate (*triangle*); cosolute-free pH buffer, ~0.1 M phosphate (*star*); sucrose, 0.1 M borate, pH 8.3 (*open circle*); glycerol, 0.1 M borate, pH 8.3 (*open square*); and ethylene glycol, 0.1 M borate, pH 8.3 (*open diamond*). PEG-200 and cosolute-free buffer values are from Table 3, where corresponding pH values (7.3–7.9) are tabulated. The values of k and error bars for sucrose, glycerol, and ethylene glycol are taken from Sawicki and Khaleque (1983).

with those from Sawicki and Khaleque (1983), were fit to Eq. 22 (except for the outlier value noted for the highest weight percent, 49%, ethylene glycol solution in Fig. 5, which was omitted from all of the fits presented here), the fitting procedure allowing C_0, σ, $\Delta N^{\ddagger}_{obs}$, and α to vary freely in a nonlinear least-squares optimization. The results of the fitting are shown in Fig. 6. The correlation between the experimental and fitted rate constants is very good; almost all of the points lie within one or two standard deviations of a line representing perfect correlation. (The excluded 49% ethylene glycol value is shown as well to illustrate its large deviation, more than six standard deviations, from the fit obeyed by the remaining points, which justifies its exclusion from the fitting procedures. It is not clear whether the deviant value of this point, corresponding to the smallest rate constant reported by Sawicki and Khaleque, reflects a limitation of their instrument's detection abilities or a shortcoming of the fitting expression at very high osmotic strengths.) The parameter values obtained from the fit are shown in Table 4. The value of α measured here is identical to that obtained previously by Eaton et al. (1991), which is not surprising given the wide applicability of the linear free energy relation embodied in α over the range of environmental conditions tabulated by those authors.

The value of σ obtained for hemoglobin is significantly smaller than the value reported previously for myoglobin, although not knowing how strongly σ depends on temperature it is difficult to say how much of this difference results simply from the lower temperatures sampled in the myoglobin study. Given that hemoglobin is made up from myoglobin-like subunits, it seems reasonable to assume that ζ_P will be the same for both proteins. In this case, the lower σ value observed for hemoglobin suggests that a greater fraction of the protein atoms involved in conformational change is exposed to solvent in hemoglobin relative to myoglobin. Although difficult to corroborate quantitatively, this inference appears to be reasonable. The allosteric transformation is thought to involve motion of the F-helix near the heme pocket and the F-G corner, C-terminus, and C-helix of each subunit at the dimer-dimer interface, all of which are significantly exposed to solvent (Perutz, 1970; Baldwin and Chothia, 1979; Fermi et al., 1984), whereas the greatest conformational change in myoglobin is probably centered at the heme pocket (Ansari et al., 1992), which is plausibly less solvent-accessible than the interfacial surfaces in hemoglobin.

The fitting described above for Eq. 22 was next repeated with the fractional exponent viscosity expression of Eq. 6 replacing the σ expression to obtain

$$k_{R_0 \rightarrow T_0} = C_0\, \eta^{-\nu}\, a_1^{\Delta N^{\ddagger}_{obs}} ([H^+]/[H^+]_0)^{2\alpha} \qquad (23)$$

A value of $\nu = 0.56 \pm 0.03$ was obtained by fitting the experimental rate constants shown in Fig. 6 to Eq. 23, the values of C_0, α, and $\Delta N^{\ddagger}_{obs}$ (Table 4) remaining the same within experimental error as those found from Eq. 22 except for a trivial change in the constant factor C_0 reflecting the change in units. The ν value obtained here is within the range of ν values typically reported for proteins, 0.4–0.6. Comparing the two approaches to treating viscosity effects embodied in Eqs. 6 and 8 and incorporated into Eqs. 23 and 22, respectively, the quality of the fits (χ^2) obtained from the latter two equations were similar; therefore, these data cannot distinguish between the validity of the two viscosity treatments. In any event, both approaches yield the same qualitative interpretation: the allosteric transition in hemoglobin involves intraprotein motions that are partially

TABLE 4 Kinetic parameters obtained from fits of experimental $R_0 \rightarrow T_0$ rate constants to Eqs. 22–24

Eq. No.	Viscosity dependence	C (s^{-1}) $\times 10^{-4}$	α	σ	ν	$\Delta N^{\ddagger}_{obs}$	χ^2
22	$(\sigma + \eta)^{-1}$	3.5 ± 0.4	0.17 ± 0.02	2.0 ± 0.3	—	9.3 ± 0.3	0.028 ± 0.006
23	$\eta^{-\nu}$	1.2 ± 0.1	0.17 ± 0.02	—	0.56 ± 0.03	9.1 ± 0.3	0.021 ± 0.005
24	$\eta^{-\nu(M)}$	1.2 ± 0.1	0.17 ± 0.02	—	—	8.6 ± 0.4	0.031 ± 0.005

shielded from coupling to solvent damping forces by protein atoms that are not involved in the conformational change.

Finally, addressing the concerns raised by Yedgar et al. (1995) regarding the apparent protein independence of ν values, we applied a third fitting procedure in which the ν value for each cosolute was fixed to the empirical ν value given by Eq. 7

$$k_{R_0\rightarrow T_0} = C_0\eta^{-\nu(M)}a_1^{\Delta N^{\ddagger}_{obs}}([H^+]/[H^+]_0)^{2\alpha} \qquad (24)$$

This last procedure gave fitted values for the remaining parameters that were not significantly different from those found from the fitting procedures for Eqs. 22 and 23, as shown in Table 4. This result is not surprising given that the empirically assigned ν values for the cosolutes used here, 0.40, 0.54, 0.59, and 0.45 for sucrose, glycerol, ethylene glycol, and PEG-200, respectively, cluster closely around the fitting-derived value, 0.56, describing the aggregate viscosity dependence for the set of cosolutes. However, this observation does allow us to rule out the possibility that the inhomogeneous solvent microviscosity effects reported by Yedgar et al. (1995), and proposed earlier by Sawicki and Khaleque (1983), contributed significantly to the dependence of rate constant on water activity reported here (both activity and microviscosity effects are expected to be sensitive to the molecular weight of the cosolute). It appears that larger variations in cosolute molecular weight than those used here may be required to observe such microviscosity effects.

The agreement observed in Fig. 6 between experimental data for the allosteric transition in hemoglobin and the kinetic expression shown in Eq. 22 supports the validity of the transition state theory expression for the effect of water activity presented in Eq. 21. The size of this effect is measured by the value of $\Delta N^{\ddagger}_{obs}$, the observed number of additional water molecules needed to stabilize the allosteric transition state during the $R_0 \rightarrow T_0$ transition. The correlation found here between the kinetics of conformational change and water activity appears to be robust in the sense that the values of $\Delta N^{\ddagger}_{obs}$ shown in Table 4 are not significantly sensitive to the choice of empirical viscosity function (although such functions tend to produce somewhat similar viscosity dependences with the parameter values typical for proteins, such as those inferred in this work).

Inferring a value of $\Delta N^{\ddagger}_{w}$, the true activation hydration number, from the $\Delta N^{\ddagger}_{obs}$ values presented in Table 4 requires knowledge of K_P values for the interactions all of the cosolutes considered with those areas of the protein surface that are additionally exposed to solvent in the transition state (see discussion of Eq. 21). Such K_P values do not seem to be available for the R $\rightarrow$ T transition in hemoglobin, but the evidence discussed below suggests that they are small enough that $\Delta N^{\ddagger}_{obs} \sim 9$ can serve as a useful preliminary estimate of $\Delta N^{\ddagger}_{w}$. However, until more information about protein-cosolute interactions is available, this number must more strictly be regarded as a lower limit on $\Delta N^{\ddagger}_{w}$. The approximation $K_P \approx 0$ appears to be reasonable for a large polyether like PEG-200, which cannot donate hydrogen bonds, but may be more severe for small polyol cosolutes that can both donate and accept hydrogen bonds. Courtenay et al. (2000) measured the relative partitioning of small cosolutes between bulk aqueous solvent and the local solvent domain near the protein surface (roughly a monolayer) of bovine serum albumin (BSA). They measured a value of $K_P = 0.83$ for glycerol, which is not much smaller than the value expected for a randomly distributed cosolute. In contrast, those authors measured a value of 0.14 for betaine, which they concluded was the most excluded of the cosolutes studied for BSA. The nonzero K_P value measured for BSA suggests that glycerol (and similar small cosolutes) may also replace water molecules to some extent in the local domain around hemoglobin. To the extent that it does and this replacement differs between the R-state and transition-state conformations of the protein, a measurement of $\Delta N^{\ddagger}_{w}$ using glycerol as a cosolute will tend to be an underestimate (Eq. 21). Using the K_P value measured for glycerol, Courtenay et al. calculated that the value of ΔN_w for a BSA reaction would be underestimated by a factor of $(1 - K_P)^{-1} \sim 6$ in osmotic stress measurements using this cosolute. In that case, measurements with cosolutes, such as betaine, that by their chemical nature are less likely to interact directly with protein surfaces, would provide a better estimate. Although, as mentioned above, K_P values for hemoglobin-cosolute interactions do not seem to be available to evaluate this possibility for the present case, equilibrium osmotic stress effects in hemoglobin are generally observed to be rather insensitive to solute identity (Colombo et al., 1992), e.g., betaine versus triethylene glycol (Parsegian et al., 2000). Those hemoglobin results appear to preclude the presence of protein-solute interactions as large as those observed in BSA, and suggest that hydration changes associated with the R $\rightarrow$ T transition tend to be localized to pockets or cavities, presumably associated with the dimer-dimer interface, that are sterically inaccessible to cosolutes. It seems reasonable to expect that hydration changes between the reacting and transition states will be located in roughly the same regions as hydration changes between the reaction end states. If so, one would expect that hydration changes in the transition state are similarly concentrated in regions from which cosolutes are sterically excluded. On that basis, measurements of kinetic osmotic stress effects in hemoglobin would be expected to be relatively independent of cosolute-protein interactions. Further kinetic osmotic stress experiments will be needed to test this assumption.

It is interesting to compare the value of $\Delta N^{\ddagger}_{w}$ inferred here, ~9, with the number of water molecules that are lost by the tetramer on going from the R to the T quaternary state, $\Delta N_w \sim -60$. In picking up these additional waters on moving from the R to the transition state conformation, the

tetramer has acquired a total of ~70 "excess" water molecules that are presumably shed as it goes from the transition state to the equilibrium hydration of the T-state tetramer. The magnitude of the ratio $\Delta N_w^{\ddagger}/\Delta N_w$, 0.15, is similar to the α value used to estimate the effects of other perturbations, such as pH or ligand binding, on the transition state free energy from their effects on the end state free energies. However, the parameter α is intended to describe the transition state free energy as a linear interpolation between the reactant and product free energies, with the limit $\alpha = 0$ corresponding to a completely reactant-like transition state and $\alpha = 1$ denoting a completely product-like state (Szabo, 1978). The sign of the ratio $\Delta N_w^{\ddagger}/\Delta N_w$ is negative, which would imply an α value that is inverted in sign from that observed for other perturbations. In other words, unlike other allosteric effectors, the effect of water on the transition state is not intermediate between its effect on the end states; rather, it is larger than the end-state effects. Eaton et al. (1991) used the value of 0.2 for α, obtained by examining the kinetic effects of a variety of allosteric perturbations, to conclude that the transition state is more R-like than T-like, implying that the transition state lies closer to the R state than the T state along the $R_0 \rightarrow T_0$ reaction coordinate. Although a negative value of α appears to lie outside of the assumptions underlying the linear free energy approach to describing transition states (Szabo, 1978), the small magnitude of the value inferred from the effect of water activity seems at least consistent with a characterization of the transition state as R-like.

The special kinetic status for water activity as an allosteric effector suggested by these results may arise from the close connection of $\Delta N_w^{\ddagger}$ to the solvent-exposed area of the protein. The number of additional water molecules required to solvate the transition state is expected to be proportional to the increase in solvent-exposed area of the transition state. The positive value of $\Delta N_w^{\ddagger}$ measured here thus implies that the transition state has a greater solvent-exposed area than either equilibrium state. By using the expected covering area of a single water molecule, admittedly a rather uncertain number, we can estimate that ~100 Å^2 of additional surface area are exposed to solvent as the protein evolves from the R-conformation to the transition state. Independent experimental measurements of the transition state solvent-exposed area are not available, but Janin and Wodak (1985) carried out a theoretical calculation of the $R \leftrightharpoons T$ reaction pathway relying heavily on the assumption that the energies of protein conformations intermediate along the pathway are dominated by hydrophobic contributions, which they estimated from the surface area buried between dimers. The reaction pathway calculated from this simplified model had a minimum in buried surface area that occurred at a conformation closer to R than to the T quaternary structure, a finding that can be interpreted as theoretical support for an R-like transition state (Eaton et al., 1991). In this regard, theoretical evidence for an R-like transition state also comes from normal mode analyses of hemoglobin R and T conformations (Mouawad and Perahia, 1996). The minimum calculated by Janin and Wodak, ~400 Å^2 lower than the R-state buried surface area, strongly suggests that the corresponding total solvent-exposed surface area goes through a maximum at this "transition state" conformation. If the differences between equilibrium R- and T-state solvent-exposed areas are a guide (Lesk et al., 1985), then the increase in solvent-exposed surface area of the transition state relative to the R-state estimated from this calculation will be some fraction between 0.2 and 0.7 of the 400 Å^2 change in surface area buried at the dimer-dimer interface, the precise fractional value depending on how much solvent exclusion is assumed to accompany compensating changes in buried surface area elsewhere in the protein. The increase in solvent-exposed surface area, 100–300 Å^2, estimated from the reaction path calculation in this way is thus consistent with the area estimated from the value of $\Delta N_w^{\ddagger}$ measured in this study. This agreement between theory and experiment, albeit within rather wide error bounds, tends to support the validity of Janin and Wodak's proposal that hydrophobic energies based on the dimer-dimer buried surface area are a useful guide in estimating the stabilities of protein conformations along the reaction path, which further underscores the importance of the solvent-exposed surface area as a determining factor in the free energy of the transition state. From this point of view, one would expect $\Delta N_w^{\ddagger}$ values to be generally positive for allosteric reactions, i.e., that transition states have higher hydration requirements than end states, as observed here for hemoglobin, because in this view it is the balance between hydration energies and hydrophobic contact energies, constrained by intraprotein steric repulsions as the protein conformation evolves along the reaction path, that largely determines the free energy barrier for the allosteric transition.

A slowing of protein conformational change under osmotic stress, also in the face of increased thermodynamic driving force, has been observed in the photoreactions of rhodopsin. The time constant for formation of the metarhodopsin II intermediate from metarhodopsin I increases from 1.2 to 1.6 ms on addition of 1 osmolal sucrose or glycerol, despite the release of 20 water molecules during the transition shifting the equilibrium toward metarhodopsin II (Mitchell and Litman, 1999). A hydration difference was not reported for the rhodopsin transition state, but the kinetic result implies that $\Delta N_w^{\ddagger} > 0$. Although observations from only two proteins cannot be conclusive, the rhodopsin results do add further experimental support to the theoretically appealing notion that the kinetic barriers to allosteric conformational changes in proteins will generally be correlated with maxima in the number of water molecules required for hydration.

More experiments will be needed to test the generality of these findings concerning the effect of water activity on the rate of protein conformational change in allostery. An issue

that needs to be explored in hemoglobin in particular is the influence of other allosteric effectors on the kinetic consequences of water activity reported here. Colombo and Seixas (1999) examined hemoglobin that had been stripped of effectors versus either Cl^-- or DPG-bound hemoglobin. They found that only ~25 additional water molecules bound to the tetramer during the deoxy → oxy transition in the absence of anions, as opposed to the ~72 water molecules that bound in the presence of >50 mM Cl^- or 15 μM DPG. Those equilibrium findings for ΔN_w suggest that kinetic experiments controlling for the presence of anion effectors may detect corresponding changes in $\Delta N_w^{\ddagger}$ as a function of effector molecule concentration.

CONCLUSIONS

This work has investigated the effect of PEG, an osmolyte that shifts the R ↔ T allosteric equilibrium in favor of low-affinity T, on the relaxation kinetics of human hemoglobin after CO photolysis. A global kinetic analysis of nanosecond time-resolved absorption data showed that PEG decreases the rate constants associated with both quaternary and tertiary structural relaxations. An analysis of rate constants for the $R_0 \rightarrow T_0$ allosteric transition obtained from these data and those of others showed that both viscosity and osmotic effects make important contributions to slowing the conformational change. Examining the variation of rate constant with water activity allowed us to determine a value for the increment in hydration for the transition state relative to the reacting R state: $\Delta N_w^{\ddagger} \approx 9$ water molecules. This number implies that the structure of the transition state exposes ~100 $Å^2$ of additional surface area to the solvent, a result that appears to be in reasonable agreement with the surface area change estimated from model calculations. However, in the absence of data on how perfectly the cosolutes considered here are excluded from the layer of molecules solvating the increased solvent-exposed area of the allosteric transition state, the value reported here for $\Delta N_w^{\ddagger}$ must be regarded as a lower limit on the true value.

Although this is to our knowledge the first report of a $\Delta N_w^{\ddagger}$ value for an allosteric protein, previously reported theoretical and experimental results discussed above are also consistent with the proposal that nonnegative values of $\Delta N_w^{\ddagger}$ may be a general feature of protein allostery. In any event, the results presented here demonstrate the importance of considering osmotic effects when studying the kinetics of protein conformational change in the presence of cosolutes such as buffers and viscous solutes.

We thank Ólöf Einarsdóttir, Jim Lewis, and Gene Switkes for many helpful discussions, and Editorial Board member Tom Record for guidance on the effect of protein-cosolute interactions on osmotic stress measurements.

Financial support for this work was provided by the National Institute of General Medical Sciences Grant (NIH) GM38549 and the Marilyn C. Davis Scholarship Fund.

REFERENCES

Alpert, B., S. El Mohsni, L. Lindqvist, and F. Tfibel. 1979. Transient effects in the nanosecond laser photolysis of carboxyhemoglobin: "cage" recombinations and spectral evolution of the protein. *Chem. Phys. Lett.* 64:11–16.

Ansari, A., C. M. Jones, E. R. Henry, J. Hofrichter, and W. A. Eaton. 1992. The role of solvent viscosity in the dynamics of protein conformational changes. *Science.* 256:1796–1798.

Antonini, E., and M. Brunori. 1971. Hemoglobin and Myoglobin in Their Reactions with Ligands. North-Holland, Amsterdam.

Arakawa, T., and S. N. Timasheff. 1982. Stabilization of protein structure by sugars. *Biochemistry.* 21:6536–6544.

Arakawa, T., and S. N. Timasheff. 1985. Mechanism of poly(ethylene glycol) interaction with proteins. *Biochemistry.* 24:6756–6762.

Baldwin, J., and C. Chothia. 1979. Hemoglobin: the structural changes related to ligand binding and its allosteric mechanism. *J. Mol. Biol.* 129:175–220.

Barshtein, G., A. Almagor, S. Yedgar, and B. Gavish. 1995. Inhomogeneity of viscous aqueous solutions. *Phys. Rev. E.* 52:555–557.

Beece, D., L. Eisenstein, H. Frauenfelder, D. Good, M. C. Marden, L. Reinisch, A. H. Reynolds, L. B. Sorensen, and K. T. Yue. 1980. Solvent viscosity and protein dynamics. *Biochemistry.* 19:5147–5157.

Björling, S. C., R. A. Goldbeck, S. J. Paquette, S. J. Milder, and D. S. Kliger. 1996. Allosteric intermediates in hemoglobin. 1. Nanosecond time-resolved circular dichroism spectroscopy. *Biochemistry.* 35: 8619–8627.

Colombo, M. F., D. C. Rau, and V. A. Parsegian. 1992. Protein solvation in allosteric regulation: a water effect on hemoglobin. *Science.* 256: 655–659.

Colombo, M. F., and F. A. V. Seixas. 1999. Novel allosteric conformation of human Hb revealed by the hydration and anion effects on O_2 binding. *Biochemistry.* 38:11741–11748.

Courtenay, E. S., M. W. Capp, C. F. Anderson, and M. T. Record. 2000. Vapor pressure osmometry studies of osmolyte-protein interactions: implications for the action of osmoprotectants in vivo and for the interpretation of "osmotic stress" experiments in vitro. *Biochemistry.* 39:4455–4471.

Doster, W. 1983. Viscosity scaling and protein dynamics. *Biophys. Chem.* 17:97–103.

Duddell, D. A., R. J. Morris, and J. T. Richards. 1979. Ultra-fast recombination in nanosecond laser photolysis of carbonylhemoglobin. *J. Chem. Soc. Chem. Commun.* 75–76.

Eaton, W. A., E. R. Henry, and J. Hofrichter. 1991. Application of linear free energy relations to protein conformational changes: the quaternary structural change of hemoglobin. *Proc. Natl. Acad. Sci. U.S.A.* 88: 4472–4475.

Esquerra, R. M., R. A. Goldbeck, S. H. Reaney, A. M. Batchelder, Y. Wen, J. W. Lewis, and D. S. Kliger. 2000. Multiple geminate ligand recombinations in human hemoglobin. *Biophys. J.* 78:3227–3239.

Fermi, G., M. F. Perutz, B. Shaanan, and R. Fourme. 1984. The crystal structure of human deoxyhemoglobin at 1.74 Å resolution. *J. Mol. Biol.* 175:159–174.

Findsen, E. W., J. M. Friedman, and M. R. Ondrias. 1988. Effect of solvent viscosity on the heme-pocket dynamics of photolyzed (carbonmonoxy)-hemoglobin. *Biochemistry.* 27:8719–8724.

Friedman, J. M., and K. B. Lyons. 1980. Transient Raman study of CO-hemoprotein photolysis: origin of the quantum yield. *Nature.* 284: 570–572.

Friedman, J. M., D. L. Rousseau, and M. R. Ondrias. 1982. Time-resolved resonance Raman studies of hemoglobin. *Annu. Rev. Phys. Chem.* 33: 471–491.

Gavish, B. 1980. Position-dependent viscosity effects on rate coefficients. *Phys. Rev. Lett.* 44:1160–1163.

Gegiou, D., K. A. Muszkat, and E. Fischer. 1968. Temperature dependence of photoisomerization. VI. The viscosity effect. *J. Am. Chem. Soc.* 90:12.

Geraci, G., L. J. Parkhurst, and Q. H. Gibson. 1969. Preparation and properties of α- and β-chains from human hemoglobin. *J. Biol. Chem.* 244:4664–4667.

Goldbeck, R. A., and D. S. Kliger. 1993. Nanosecond time-resolved absorption and polarization dichroism spectroscopies. *Methods Enzymol.* 226:147–177.

Goldbeck, R. A., S. J. Paquette, S. C. Björling, and D. S. Kliger. 1996. Allosteric intermediates in hemoglobin. 2. Kinetic modeling of HbCO photolysis. *Biochemistry.* 35:8628–8639.

Henry, E. R., and J. Hofrichter. 1992. Singular value decomposition: applications to experimental data. *Methods Enzymol.* 210:129–193.

Hofrichter, J., J. H. Sommer, E. R. Henry, and W. A. Eaton. 1983. Nanosecond absorption spectroscopy of hemoglobin: elementary processes in kinetic cooperativity. *Proc. Natl. Acad. Sci. U.S.A.* 80: 2235–2239.

Janin, J., and S. J. Wodak. 1985. Reaction pathway for the quaternary structure change in hemoglobin. *Biopolymers.* 24:509–526.

Jayaraman, V., K. R. Rodgers, I. Mukerji, and T. G. Spiro. 1995. Hemoglobin allostery: resonance Raman spectroscopy of kinetic intermediates. *Science.* 269:1843–1848.

Kliger, D. S., J. W. Lewis, and C. E. Randall. 1990. Polarized Light in Optics and Spectroscopy. Academic, San Diego.

Kramers, H. A. 1940. Brownian motion in a field of force and the diffusion model of chemical reaction. *Physica.* 7:284–304.

Lavalette, D., and C. Tetreau. 1988. Viscosity-dependent energy barriers and equilibrium conformational fluctuations in oxygen recombination with hemerythrin. *Eur. J. Biochem.* 177:97–108.

Lee, J. C., and L. L. Y. Lee. 1981. Preferential solvent interactions between proteins and polyethylene glycols. *J. Biol. Chem.* 256:625–631.

Lesk, A. M., J. Janin, S. Wodak, and C. Chothia. 1985. Hemoglobin: the surface buried between the $\alpha_1\beta_1$ and $\alpha_2\beta_2$ dimers in the deoxy and oxy structures. *J. Mol. Biol.* 183:267–270.

Lewis, J. W., G. G. Yee, and D. S. Kliger. 1987. Implementation of an optical multichannel analyzer controller for nanosecond flash photolysis measurements. *Rev. Sci. Instrum.* 58:939–944.

LiCata, V. J., and N. M. Allewell. 1998. Measuring hydration changes of proteins in solution: applications of osmotic stress and structure-based calculations. *Methods Enzymol.* 295:42–62.

McKinnie, R. E., and J. S. Olson. 1981. Effects of solvent composition and viscosity on the rates of CO binding to heme proteins. *J. Biol. Chem.* 256:8928–8932.

Mitchell, D. C., and B. J. Litman. 1999. Effect of protein hydration on receptor conformation: decreased levels of bound water promote metarhodopsin II formation. *Biochemistry.* 38:7617–7623.

Mouawad, L., and D. Perahia. 1996. Motions in hemoglobin studied by normal mode analysis and energy minimization: evidence for the existence of tertiary T-like, quaternary R-like intermediate structures. *J. Mol. Biol.* 258:393–410.

Murray, L. P., J. Hofrichter, E. R. Henry, and W. A. Eaton. 1988. Time-resolved optical spectroscopy and structural dynamics following photodissociation of carbonmonoxyhemoglobin. *Biophys. Chem.* 29:63–76.

Okada, A. 2000. Fractional power dependence of the mean lifetime of a first order reaction on the time scale of environmental relaxation in the slow diffusion limit. *J. Chem. Phys.* 112:8595–8604.

Parsegian, V. A., R. P. Rand, M. F. Colombo, and D. C. Rau. 1994. Water at the macromolecular surface: solvation energy and functional control. *Adv. Chem. Series.* 235:177–196.

Parsegian, V. A., R. P. Rand, and D. C. Rau. 1995. Macromolecules and water: probing with osmotic stress. *Methods Enzymol.* 259:43–93.

Parsegian, V. A., R. P. Rand, and D. C. Rau. 2000. Osmotic stress, crowding, preferential hydration, and binding: a comparison of perspectives. *Proc. Natl. Acad. Sci. U.S.A.* 97:3987–3992.

Perutz, M. F. 1970. Stereochemistry of cooperative effects in hemoglobin. *Nature.* 228:726–734.

Perutz, M. F. 1992. The significance of the hydrogen bond in physiology. *In* The Chemical Bond: Structure and Dynamics. A. Zewail, editor. Academic, San Diego. 17–30.

Perutz, M. F., J. E. Ladner, S. R. Simon, and C. Ho. 1974. Influence of globin structure on the state of the heme. I. Human deoxyhemoglobin. *Biochemistry.* 13:2163–2172.

Pollak, E. 1996. Theory of activated rate processes. *In* Dynamics of Molecules and Chemical Reactions. R. E. Wyatt and J. Z. H. Zhang, editors. Dekker, New York. 617–669.

Rodgers, K. R., C. Su, S. Subramaniam, and T. G. Spiro. 1992. Hemoglobin R $\rightarrow$ T structural dynamics from simultaneous monitoring of tyrosine and tryptophan time-resolved UV resonance Raman signals. *J. Am. Chem. Soc.* 114:3697–3709.

Rosenberg, A., K. Ng, and M. Punyiczki. 1989. Activity and viscosity effects on the structural dynamics of globular proteins in mixed solvent systems. *J. Mol. Liquids.* 42:31–43.

Sawicki, C. A., and Q. H. Gibson. 1976. Quaternary conformational changes in human hemoglobin studied by laser photolysis of carboxyhemoglobin. *J. Biol. Chem.* 251:1533–1542.

Sawicki, C. A., and M. A. Khaleque. 1983. Laser photolysis study of conformational change rates for hemoglobin in viscous solutions. *Biophys. J.* 44:191–199.

Schlitter, J. 1988. Viscosity dependence of intramolecular activated processes. *Chem. Phys.* 120:187–197.

Scott, T. W., and J. M. Friedman. 1984. Tertiary-structure relaxation in hemoglobin: a transient Raman study. *J. Am. Chem. Soc.* 106: 5677–5687.

Shapiro, D. B., R. A. Goldbeck, D. Che, R. M. Esquerra, S. J. Paquette, and D. S. Kliger. 1995. Nanosecond optical rotatory dispersion spectroscopy: application to photolyzed hemoglobin-CO kinetics. *Biophys. J.* 68:326–334.

Stock, J. B., B. Rauch, and S. Roseman. 1977. Periplasmic space in *Salmonella typhimurium* and *Escherichia coli. J. Biol. Chem.* 252: 7850–7861.

Szabo, A. 1978. Kinetics of hemoglobin and transition state theory. *Proc. Natl. Acad. Sci. U.S.A.* 75:2108–2111.

Weast, R. C. 1972. Handbook of Chemistry and Physics. Chemical Rubber Publishing, Cleveland.

Yedgar, S., C. Tetreau, B. Gavish, and D. Lavalette. 1995. Viscosity dependence of O_2 escape from respiratory proteins as a function of cosolvent molecular weight. *Biophys. J.* 68:665–670.

Zwanzig, R. 1992. Dynamical disorder: passage through a fluctuating bottleneck. *J. Chem. Phys.* 97:3587–3589.